Chemical Science

ROYAL SOCIETY OF CHEMISTRY

EDGE ARTICLE

View Article Online
View Journal | View Issue

Cite this: *Chem. Sci.*, 2021, **12**, 7003

All publication charges for this article have been paid for by the Royal Society of Chemistry

Library construction of stereochemically diverse isomers of spirooliganin: their total synthesis and antiviral activity†

Ru-Bing Wang,‡[a] Shuang-Gang Ma, ‡*[a] Cooper S. Jamieson,‡[b] Rong-Mei Gao,[c] Yun-Bao Liu,[a] Yong Li, [a] Xiao-Jing Wang,[a] Yu-Huan Li,[c] Kendall N. Houk, *[b] Jing Qu*[a] and Shi-Shan Yu *[a]

Received 4th March 2021
Accepted 9th April 2021

DOI: 10.1039/d1sc01277k

rsc.li/chemical-science

The construction of libraries of stereoisomers of natural products serves as an important approach to investigating the correlation between the stereostructure and biological activity. However, the total synthesis and isomerzation of polycyclic scaffolds with multiple chrial centers are rare. Spirooliganin (**1**), a new skeleton natural product isolated from the plant *Illicium oligandrum*, was structurally characterized by comprehensive analysis of NMR spectroscopic data and ECD which revealed an unprecedented 5–6–6–7 polycyclic framework with six chiral centers. Here we report a 17-step total synthesis to prepare a library of stereochemically diverse isomers of spirooliganin, including 16 diastereoisomers and 16 regioisomers. In addition to a regioselective hetero-Diels–Alder cycloaddition, the synthetic strategy involves a photo-induced stereoselective Diels–Alder reaction, which gives only the abnormal *trans*-fused product as rationalized by density functional theory calculations. Preliminary biological evaluation showed that spirooliganin and regioisomers **39** exhibited potent inhibition of Coxsackievirus B3. It also revealed the pharmacophore effect of the D-ring (16*R*,18*R*,24*R*, and 26*R*) for their antiviral activities.

Introduction

Natural products continue to be a major source of novel lead compounds or pharmacophores for medicinal chemistry due to their diverse structure and biological activities. Bioactive natural products often possess one or multiple chiral centers and spatially defined arrangements of functional groups. Given the important relationship between stereochemistry and bioactivity, the creation of stereoisomer libraries of natural products is envisaged to maximally screen the potential of novel frameworks in drug discovery.

Examples of the construction of stereoisomer libraries of natural products containing multiple chiral centers has been reported in the past few decades, such as annonaceous acetogenins, a class of fatty acid-derived natural products from members of the *Annonaceae* family,[1–4] cladosporin, an isocoumarin-based metabolite from fungus,[5] spirotryptostatin, a prenyl-containing alkaloid from *Aspergillus fumigatus*,[6–8] and cocaine, a member of the tropane alkaloids isolated from the leaves of *Erythroxylon coca*.[9] However, stereoisomeric variation in these studies was limited to scaffolds with long carbon-chain skeletons or polyketide macrolides[10,11] that contain multiple oxygenated chiral centers, or molecules with two vicinal stereogenic centers.[9,12–15] Due to the synthetic challenge, there exists no stereoisomer library constructed for natural products with a rigid, polycyclic fused ring scaffold and multiple resulting stereocenters. Thus, the stereostructure–activity relationship (SSAR) for many of these natural products is unknown.

Inspired by the potential antiviral activity of prenylated C6–C3 compounds,[16–19] which are characteristic constituents of plants from the genus *Illicium*, we isolated and characterized spirooliganin (**1**) from the stem bark of *I. oligandrum*.[20] The compound **1** features an unprecedented linear tetracycle (6–6–6–7, rings B, C, D, and E, Fig. 1). Remarkably, this molecule exhibits potent activity against Coxsackievirus B3 (CVB3), with an IC_{50} of 2.1 μM and a selectivity index (SI) value of 5.2. Here we report the construction of a library of stereoisomers of

[a]*State Key Laboratory of Bioactive Substance and Function of Natural Medicines, Institute of Materia Medica, Chinese Academy of Medical Sciences and Peking Union Medical College, No.1 Xian Nong Tan Street, Beijing, 100050, People's Republic of China. E-mail: mashuanggang@imm.ac.cn; qujing@imm.ac.cn; yushishan@imm.ac.cn*

[b]*Department of Chemistry and Biochemistry, University of California, Los Angeles, California 90095, USA. E-mail: houk@chem.ucla.edu*

[c]*Institute of Medicinal Biotechnology, Chinese Academy of Medical Sciences and Peking Union Medical College, No. 1 Tian Tan Xi Li, Beijing, 100050, People's Republic of China*

† Electronic supplementary information (ESI) available. CCDC 2009862, 2009865, 2009868, 2009871 and 2009873. For ESI and crystallographic data in CIF or other electronic format see DOI: 10.1039/d1sc01277k

‡ These authors contributed equally to this work.

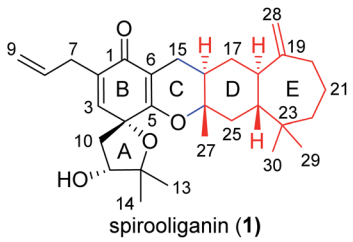

Fig. 1 Structure of spirooliganin, a novel prenylated C6–C3 compound, isolated from *I. oligandrum*.

spirooliganin, including 16 diastereoisomers and 16 regioisomers, *via* a 17-step total synthesis. The synthetic strategy involves a regioselective hetero-Diels–Alder cycloaddition and an abnormal photochemical *trans*-selective Diels–Alder reaction, which has been rationalized by density functional theory calculations. The antiviral activity of the stereoisomer library was evaluated against CVB3, thus revealing the relationship between the stereostructure and antiviral activities of this analogue of natural products.

Results and discussion

Structural elucidation of spirooliganin

Spirooliganin (**1**), a colorless oil, was determined to have the molecular formula $C_{30}H_{42}O_4$ on the basis of ^{13}C NMR data and the (+)-HRESIMS ion peak at *m*/*z* 467.3160 $[M + H]^+$ (calcd 467.3156), suggesting ten degrees of unsaturation. The IR spectrum displayed absorptions characteristic of hydroxy (3437 cm^{-1}) and carbonyl (1671 cm^{-1}) groups. Analysis of the ^{13}C NMR spectrum (Table S1†) with the aid of DEPT and HSQC spectra revealed the presence of four double bonds and one cross-conjugated carbonyl (δ_C 185.2) group in the downfield region (δ_C 186.0–109.0 ppm) and five methyls, eight methylenes, four methines (one oxygenated), and four quaternary carbons (three oxygenated) in the upfield region (δ_C 86.0–19.0 ppm). Analysis of the degree of unsaturation indicates the presence of

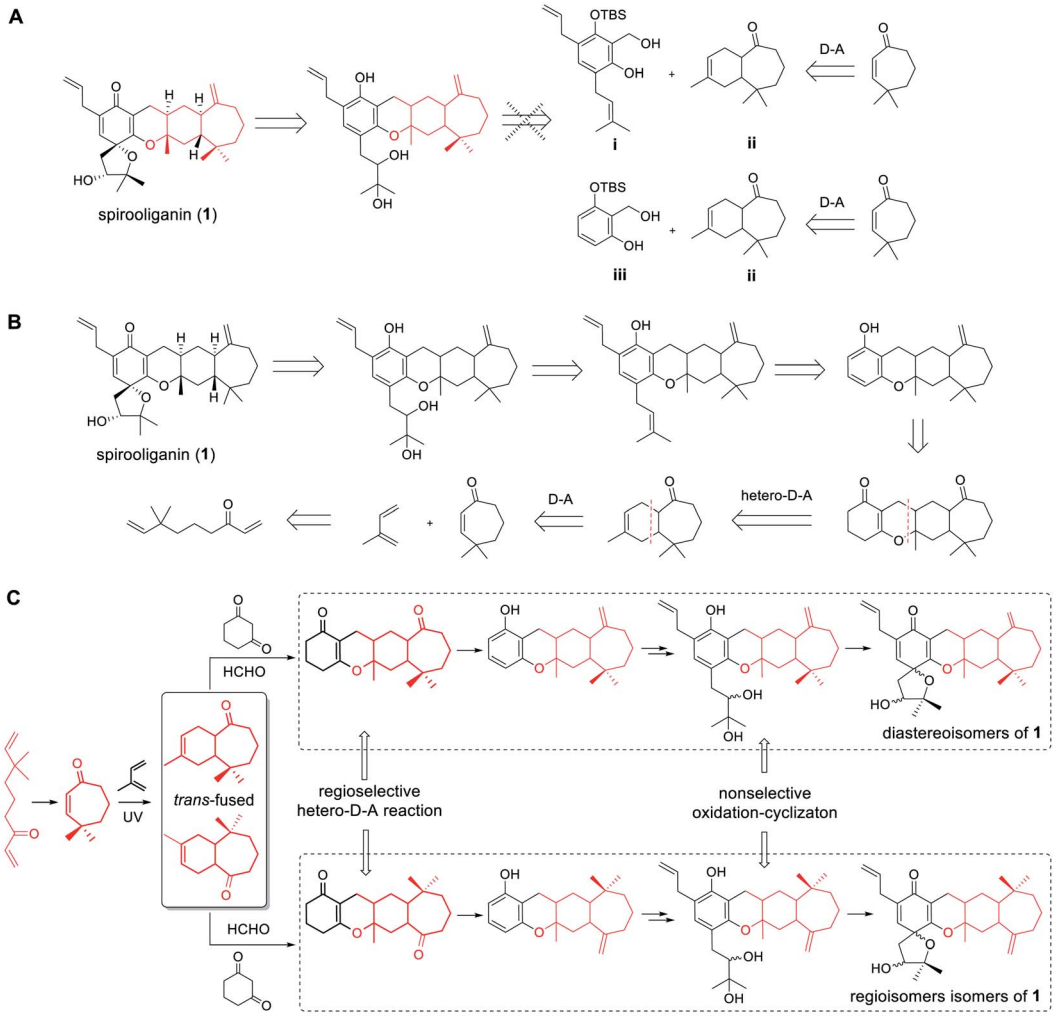

Fig. 2 General strategy and retrosynthetic analysis to produce stereochemically diverse isomers of spirooliganin (**1**). (A) Unrealized convergent retrosynthetic strategy for the construction of spirooliganin. (B) Linear retrosynthetic strategy to achieve the synthesis of isomers of spirooliganin. (C) General synthetic strategy of stereochemically diverse isomers of spirooliganin.

five rings (rings A–E) in **1**. The planar structure of **1** (Fig. 1) was determined by examination of the 2D NMR spectra, which was described as follows. Four proton-bearing structural fragments **a–d**, as depicted by bold bonds (Fig. S1A†), were readily established by interpretation of the HSQC and ^{1}H–^{1}H COSY spectra. Subsequently, a series of key HMBC correlations (Fig. S1B†) led to the determination of the planar structure of the unprecedented linearly fused tetracyclic (6–6–6–7) skeleton bearing a 1-oxaspiro[4.5]deca-6,9-dien-8-one moiety. The stereochemistry (4*R*,11*R*,16*R*,18*R*,24*R*, and 26*S*) of the chiral centers in rings A and D was unambiguously determined from the NOESY spectrum and a series of NOE experiments (Fig. S1B, S18 and S19†), as well as circular dichroism (CD) spectroscopy showing a negative Cotton effect at 255 nm and a positive Cotton effect at 309 nm. The full details of the structural elucidation can be found in the ESI.†

Strategy for the isomer library construction of spirooliganin

Structurally, spirooliganin contains a spiro-type prenylated C6–C3 unit (C1–C14, black in Fig. 1) and a himachalane-type sesquiterpenoid with a bicyclo[5.4.0]undecane skeleton (C16–C30, red in Fig. 1), which are fused through a methylene (C15) and an oxygen bridge involved in a pyran ring (C-ring). Four of the six chiral centers in spirooliganin are located on the linearly fused tetracycle (B, C, D and E rings) and two on the oxaspiro ring (A and B rings). To construct a library of spirooliganin stereoisomers for a better understanding of its SSAR, the total synthesis was envisioned to diversify the introduction of stereocenters in each step. We conceived a route to spirooliganin that succinctly delivers a wide diversity of isomers of **1** (Fig. 2).

The general synthetic strategy includes three main transformations: (1) use of a nonselective oxidation–cyclizaton to diversify the two chiral centers on the oxaspiro ring while the characteristic prenylated C6–C3 unit was retained, (2) use of a non-regioselective Diels–Alder reaction between 4,4-dimethylcyclohept-2-en-1-one and isoprene to give two kinds of cycloadditon product including regioisomers resulting from the opposite location of the exocyclic double bond and a gem-dimethyl group to maximize the isomers of **1**, and (3) use of a regioselective hetero-Diels–Alder reaction of an *o*-quinone methide with himachalane cyclohexene to obtain the linearly fused 6–6–6–7-tetracycle, which matches the basic skeleton of **1** and produces diverse stereoisomers of tetracyclic intermediates. We firstly intended to install the basic skeleton of **1** using a convergent strategy[21–23] of **i** and **ii**. However, this was not achieved, even after simplification of the starting material (**iii** to **ii**) (Fig. 2A). Therefore, we transferred to another linear

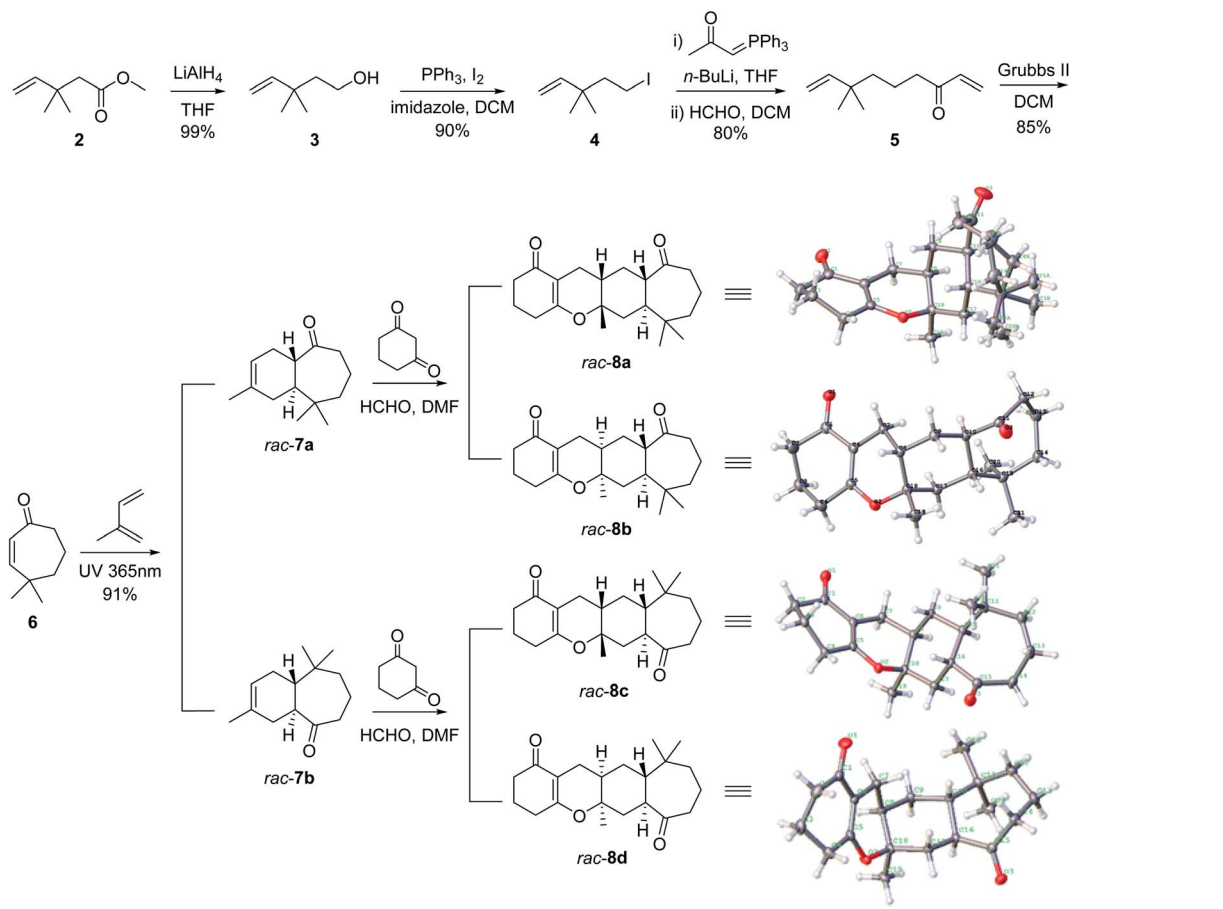

Fig. 3 Construction of the linear tetracyclic core for spirooliganin. The crystal structures of the key tetracyclic intermediates *rac*-**8a**, *rac*-**8b**, *rac*-**8c** and *rac*-**8d** were shown. *rac*-**8c** and *rac*-**8d** would be used in the same synthetic route to give spirooliganin regioisomers.

synthetic strategy to achieve the synthesis of isomers of spirooliganin (Fig. 2B). Finally, library construction of stereo isomers of spirooliganin was realized as shown in Fig. 2C.

Total syntheses of 16 diastereoisomers and 16 regioisomers of spirooliganin

The total synthesis of the polycyclic fused skeleton of spirooliganin **1** started from the commercially available methyl 3,3-dimethylpent-4-enoate **2**, which was reduced to the corresponding alcohol **3** by $LiAlH_4$ in an almost quantitative yield. A substitution reaction of **3** with iodine, imidazole and triphenylphosphine afforded **4** in 90% yield. Compound **4** was treated with *n*-BuLi and acetylmethylene triphenylphosphorane to generate an ylide intermediate,[24] which was directly used for the subsequent Wittig reaction with formaldehyde to afford α,β-unsaturated ketone **5** in the two steps with 80% yield. Compound **5** was refluxed in dichloromethane over a Grubbs II catalyst to give intramolecular ring-closure product **6** in 85% yield. Diels–Alder cycloaddition of compound **6** with isoprene (also as the solvent) under ultraviolet (UV) 365 nm irradiation generated a pair of *trans*-fused regioisomers **7a** and **7b** (Fig. 3) in a ratio of 46.8 : 53.2, which were separated by using reverse phase C18 preparative HPLC to give two pairs of racemates **7a** and **7b**.[25,26] Their structures were determined based on extensive spectroscopic evidence (Fig. S29–S40†) and also supported by the X-ray crystal structures of the products from subsequent steps (Fig. 3). The *trans*-fused product *rac*-**7a** and *rac*-**7b** served as key intermediates in the synthesis of stereoisomers and regioisomers of spirooliganin, respectively. A three-component hetero-Diels–Alder cycloaddition of *rac*-**7a**, formaldehyde and 1,3-cyclohexanedione was used to construct the 6–6–6–7 tetracyclic core according to a reported strategy.[27] Two pairs of enantiomers (*rac*-**8a** and *rac*-**8b**) were obtained (Fig. 3). To ensure the complete conversion of *rac*-**7a**, 1,3-cyclohexanedione was strictly controlled to be added in portions after the reaction was heated to 100 °C. The reaction from *rac*-**7b** was same as that from *rac*-**7a**. The hetero-Diels–Alder reaction afforded a *cis*-fused 6–6 ring system, resulting in the assembly of the key tetracyclic core, the stereochemistry of which was confirmed by X-ray crystal structures of *rac*-**8a**, *rac*-**8b**, *rac*-**8c** and *rac*-**8d** (Fig. 3, Fig. S5–S8 and Tables S21–S28†).

With the tetracyclic core in place, our attention was focused on the formation of the B ring by aromatization (Fig. 4). We expected to accomplish selective aromatization of the B ring in one step based on the slight activity difference between the α,β-unsaturated carbonyl and saturated carbonyl group. Many reported methods (Pd/C, I_2/CH_3OH, I_2/DMSO/CH_3NO_2, DDQ, and NaH/$PhSO_2CH_3$) were attempted,[27–29] such as (NaH/$PhSO_2CH_3$) reported by Xie *et al.* as a practical method for the synthesis of spirooliganones.[27] However, these attempts gave at best a trace amount of the desired

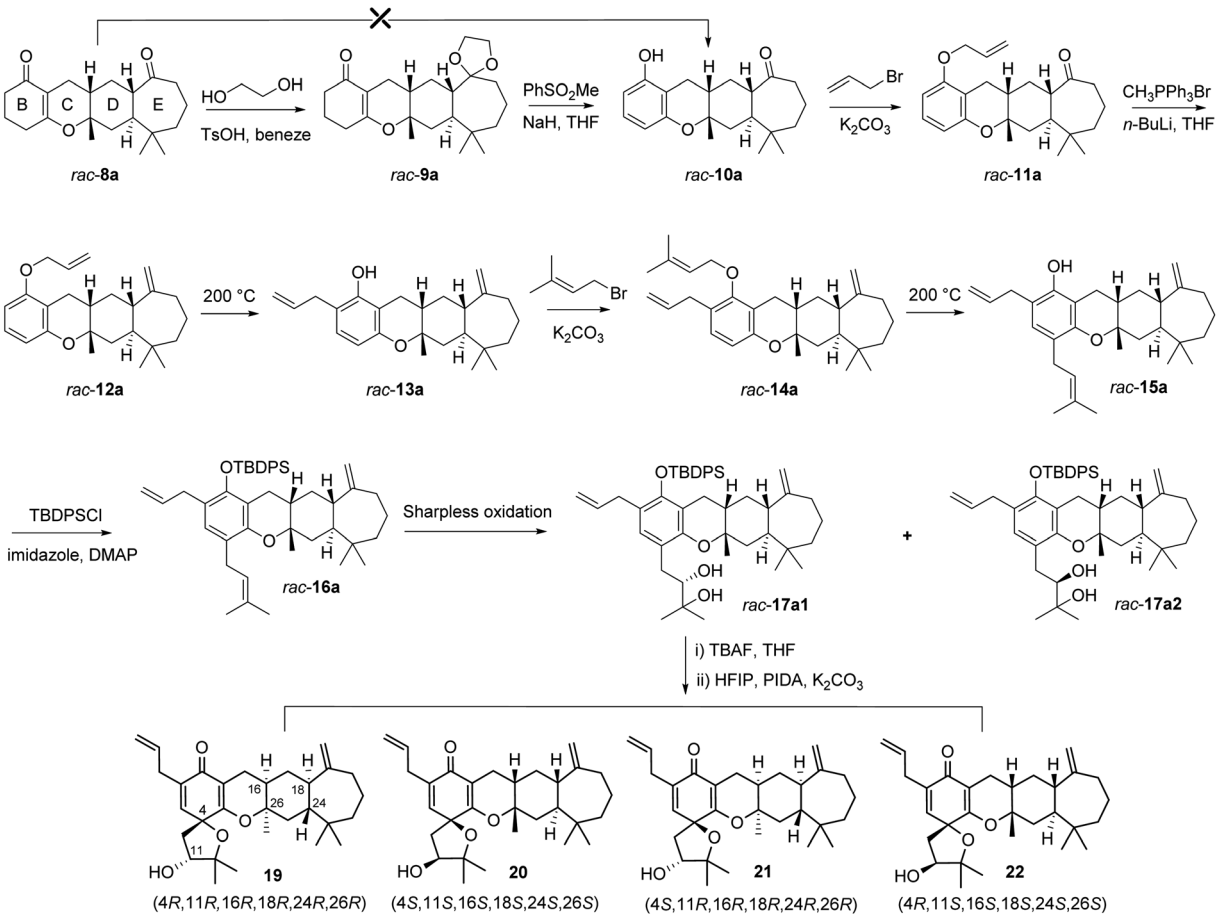

Fig. 4 Syntheses of spirooliganin diastereoisomers from *rac*-**8a**. The four diastereoisomers **19**, **20**, **21**, and **22** formed *via rac*-**17a1** were shown.

product. We speculated that this might be due to the presence of carbonyl on the seven-membered ring, which was accompanied by β-keto sulfoxide substitution when the reaction was heated to 100 °C using methyl benzenesulfinate for aromatization. We thus attempted an alternative strategy by protecting the carbonyl before aromatization. The reaction of *rac*-**8a** with glycol and trimethyloxymethane catalyzed by *p*-TsOH in benzene under violent reflux gave the corresponding protected racemates. The following aromatization of *rac*-**9a** not only converted the α,β-unsaturated ketone ring (B ring) into the corresponding phenol but also completely removed the protection of the carbonyl in two steps with 60% yield for *rac*-**10a**.

With racemic phenols *rac*-**10a** in hand, the allylic and prenyl side chains of the B ring were introduced by a general alkylation/Claisen rearrangement reaction sequence. Treatment of *rac*-**10a** with allyl bromide and K_2CO_3 in refluxing acetone efficiently delivered allylic ether *rac*-**11a** in 95% yield, followed by a Wittig reaction using the ylide of methyltriphenylphosphonium bromide to give *rac*-**12a** in 90% yield. This intermediate was converted to *o*-allylic phenols *rac*-**13a**

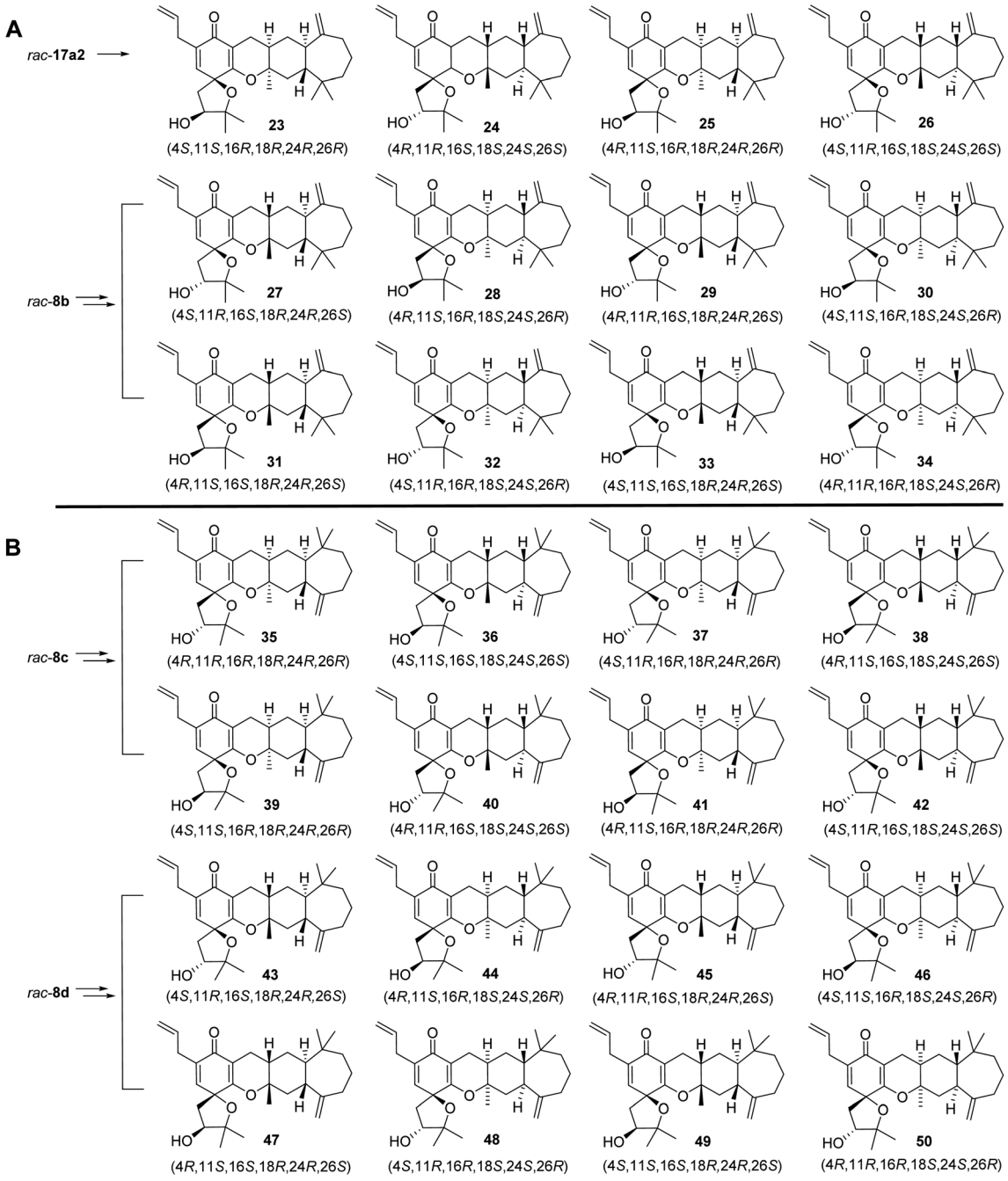

Fig. 5 Stereochemically diverse structures of isomers of spirooliganin. (A) Structures of the other 12 diastereoisomers of spirooliganin from *rac*-**17a2** and *rac*-**8b**. (B) Structures of 16 regioisomers from *rac*-**8c** and *rac*-**8d**.

with high regioselectivity in 95% yield when heated in *N*,*N*-diethylaniline. Similarly, treatment of *rac*-**13a** with prenyl bromide and K_2CO_3 in refluxing acetone efficiently produced *rac*-**14a**, which was then heated in *N*,*N*-diethylaniline to give the *p*-prenyl phenols *rac*-**15a** with high regioselectivity in 75% yield over two steps. *rac*-**15a** was protected by *tert*-butyldiphenylsilyl chloride (TBDPSCl) to produce *rac*-**16a** in 96% yield, which was subjected to Sharpless dihydroxylation with AD-mix-β at 10–15 °C for 36 h, and two pairs of racemic diols, *rac*-**17a1** (24% yield) and *rac*-**17a2** (21% yield), were generated with poor stereoselectivity and 30% conversion. We attempted to prolong the reaction time and increase the reaction temperature, but tetrol derivatives were observed as the main product from HRMS data, which may be due to the oxidation of both the isopentenyl and allyl groups. The structures of the intermediates (*rac*-**10a**, *rac*-**11a**, *rac*-**12a**, *rac*-**13a**, *rac*-**14**, and *rac*-**15a**) were confirmed by a series of 1D and 2D-NMR spectroscopic analyses (Fig. S63–S66, S79–S82, S95–S98, S111–S114, S127–S130, and S143–S146†), and their stereochemistry was the same as that of *rac*-**8a**. The stereochemistry of two pairs of racemic diols (*rac*-**17a1** and *rac*-**17a2**) was verified based on the absolute configuration of the final products **19–26** (Fig. S191–S230†).

Followed by the preparation of diols, a tandem oxidative dearomatization/cyclization reaction was adopted to construct the oxaspiro ring moiety. Treatment of *rac*-**17a1** with TBAF in THF afforded the deprotected compounds, which was reacted with iodobenzene diacetate (PIDA) in hexafluoroisopropanol (HFIP) in the presence of K_2CO_3 to generate two pairs of scalemic enantiomers **19**/**20** in 20% yield and **21**/**22** in 22% yield after purification by silica column chromatography and preparative HPLC. The enantiomers were further separated by chiral HPLC to afford single diastereoisomers, including **19**, the 26-epimer of spirooliganin.

We also prepared the other 12 diastereoisomers (**23–34**) of spirooliganin from *rac*-**17a2** and *rac*-**8b**, as well as 16 regioisomers (**35–50**) from *rac*-**8c** and *rac*-**8d** (Fig. 5). The synthetic route was same as that used for diastereoisomer synthesis from *rac*-**8a**. The structures of the final products, including the absolute configurations, were unambiguously characterized by comprehensive NMR spectroscopic analysis, a series of NOE experiments, ECD analysis, and Mosher's method (Fig. S2, S3, and S191–S369, Tables S12–S20†). Moreover, the X-ray crystal structure of a pair of enantiomers, **31** and **32**, obtained from methanol containing trace H_2O also confirmed the fascinating highly linearly fused tetracyclic (6–6–6–7) skeleton bearing a 1-oxaspiro [4.5]deca-6,9-dien-8-one moiety and six dense chiral centers (Fig. 6).

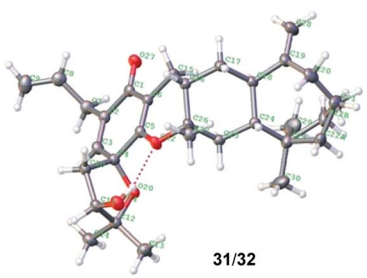

Fig. 6 The X-ray crystal structure of a pair of enantiomers **31**/**32**.

Abnormal photo-induced *trans*-selective Diels–Alder reaction

The observation that the Diels–Alder cycloaddition of compound **6** with isoprene under UV yielded 100% *trans*-fused products intrigued us to investigate the mechanism of this uncommon *trans*-photochemical cycloaddition reaction by density functional theory calculations at the ωB97X-D/def2-QZVPP//ωB97X-D/def2-TZVP level of theory. Since medium ring *trans*-cycloalkenes are known to be highly reactive in cycloadditions,[30] we hypothesized that the well-known photochemical *cis*, *trans* isomerization[31] of cycloheptenones would lead to a reactive *trans*-cycloheptenone. The reactivity of *trans*-cycloheptenones is derived from distorting the structure towards the cycloaddition transition state geometry. To verify this, we calculated the molecular orbitals (MOs) of isoprene, *cis*-, and *trans*-cycloheptenones (Fig. 7A). As has been known and explained[32] the highest occupied MO of isoprene has very similar coefficients at the two termini and is expected to react with low regioselectivity. The lowest unoccupied MOs (LUMOs) of *cis*- and *trans*-cyclohepetenones have similar orbital energies and support the idea that *trans*-cycloheptenone reactivity is distortion accelerated and not accelerated by improved orbital interactions. Alkene isomerization rotates the reacting p-orbitals out of conjugation from the ketone and results in a slight increase in the LUMO energy (+0.04 eV), despite the fact that this distortion of the alkene should intrinsically lower the alkene LUMO energy.[33]

We located the transition states for the cycloadditions of both the *cis*- and *trans*-cycloheptenones (Fig. 7B). The *cis*-cycloheptenone can react *via endo* or *exo* transition states to form two regiosomeric *cis*-fused cycloheptenone adducts. The lowest energy transition states for the regioisomeric cycloadditions are **TS-1** and **TS-2**. These transition states are *endo* and have free energies of activation of 37.1 and 37.2 kcal mol^{-1}, respectively. There is a minute (0.1 kcal mol^{-1}) preference for C-1 of isoprene to react at the β carbon of the α,β-unsaturated ketone, in agreement with the frontier molecular orbital prediction. The barriers for these cycloadditions are very high, and under mild reaction conditions would not be observed.

Isomerization of *cis*-cycloheptenone to *trans*-cycloheptenone is uphill thermodynamically by 31.9 kcal mol^{-1}. The *trans*-cycloheptenone can, similarly, undergo cycloadditions to form two regiosomeric *trans*-fused cycloheptenone adducts. In this case, the lowest energy transition states **TS-3** and **TS-4** are *exo* with respect to the cycloheptenone ketone and have low barriers of 18.1 and 18.3 kcal mol^{-1} from the *trans*-cycloheptenone, respectively. The transition states are slightly more asynchronous than those from the *cis*-cycloheptenone, but still clearly concerted. Now, there is a small preference for the opposite regioselectivity compared to the *cis*-enone reaction. The barriers for these cycloadditions of *trans*-cycloheptenone are nearly 20 kcal mol^{-1} lower than that of *cis*-cycloheptenone.

These calculations rationalize why the *cis*-fused adduct was not observed and showed the origins of stereochemistry and

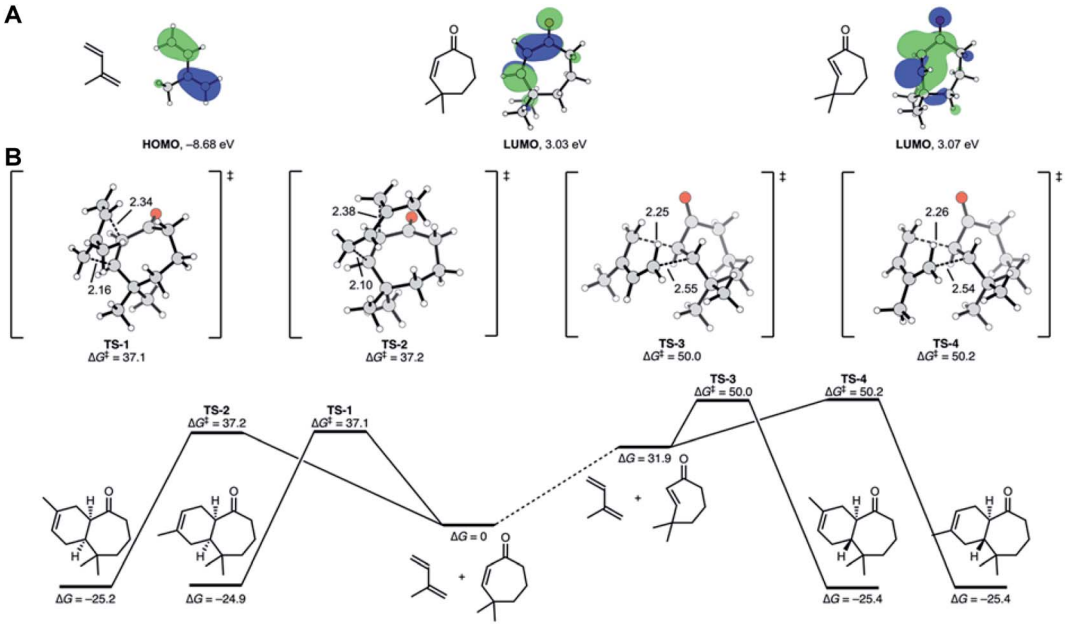

Fig. 7 DFT calculations for the intermolecular [4 + 2] cycloaddition reaction. (A) Energies and shapes of the highest occupied and lowest unoccupied molecular orbitals (HOMO and LUMO) of isoprene, *cis*-cycloheptenone and *trans*-cycloheptenone. (B) Gibbs free energy surface of cycloadditions from *cis*- and *trans*-cycloheptenones. Relative to reactants, **TS-3** and **TS-4** have low barriers of 18.1 and 18.3 kcal mol^{-1} and readily take place, whereas **TS-1** and **TS-2** are too high in energy to proceed under the experimental conditions.

regioselectivity. In short, the *cis*-cycloheptenone is unreactive in cycloadditions, but the *trans*-cycloheptenone is highly reactive and leads by a concerted cycloaddition to the *trans*-fused product.

Antiviral screening and stereostructure–activity relationship

With spirooliganin (**1**) and the 32 isomer library in hand, we were able to investigate the influence of the stereostructure on their biological activity. Compound **1** and its 16 diastereoisomers (Table 1, Groups A and B) and 16 regioisomers (Table 1, Groups C and D) were evaluated for their antiviral inhibitory activities against CVB3 in African green monkey kidney cells (Vero cells), which were infected with CVB3 and measured with CPE assay.[34] The preliminary biological study showed that compound **1** and its regioisomer **39** displayed the most potent activities against CVB3 among all the isomers, with IC_{50} values of 2.1 μM and 3.7 μM and SI values of 5.2 and 4.3, respectively, which are better than those of the positive control ribavirin (IC_{50} 1577.5 μM and SI = 5.2) but less effective than those of pleconaril. Diastereoisomer **23** and regioisomers **35**, **37**, **41**, **42**, and **47** also exhibited good inhibition against CVB3, with IC_{50} values ranging from 8.6–11.1 μM. Among the 16 diastereoisomers, compounds **21**, **23**, and **25**, with the same D-ring configuration (16*R*,18*R*,24*R*, and 26*R*), showed a better selectivity index than their corresponding enantiomers **22**, **24**, and **26**, which have the opposite D-ring configuration (16*S*,18*S*,24*S*, and 26*S*). Interestingly, a similar trend was observed for the regioisomers. With a D-ring configuration of 16*R*,18*R*,24*R*, and 26*R*, compounds **35**, **37**, **39** and **41** exhibited significant inhibitory activities against CVB3, with IC_{50} values ranging from 3.7 to 11.1 μM, although **42** also showed a similar level of activity compared to **41**. This indicated the crucial role of the D-ring configuration for their anti-CVB3 activity, while the configuration of the A-ring may be less important. Notably, natural spirooliganin (**1**) exhibited excellent inhibitory effects against CVB3 (IC_{50} 2.1 μM), while its synthetic 26-epimer (**19**) was much less active (IC_{50} > 33.3 μM), suggesting that the 26*S* configuration of the methyl group on the D-ring plays an important role in inhibiting CVB3.

Discussion

As a rich source for bioactive natural products, a number of prenylated C6–C3 compounds with diverse structures and/or significant biological activity have been isolated from different parts of the pant *I. oligandrum*.[17–20] Herein, spirooliganin (**1**), a prenylated C6–C3 compound, has been isolated from the plant stem bark and structurally characterized. It features an unprecedented linear tetracycle with six dense chiral centers and was characterized as the first example of a hybrid of spiro-type prenylated C6–C3 derivative and himachalane sesquiterpenoids (C16–C30) from *I. oligandrum*.

For the SSAR study, we applied an effective total synthesis route that maximizes isomer formations to construct a library of stereochemically diverse isomers of spirooliganin. The 17-step total synthesis started from readily available materials and included five main transformations: (1) an intramolecular ring-closure reaction to furnish 2-cycloheptenone and a photo-induced Diels–Alder cycloaddition to assemble the *trans*-fused 6–7 ring system; (2) a three-component regioselective hetero-Diels–Alder cycloaddition reaction to build the 6–6–6–7 tetracyclic core; (3) aromatization of the α,β-unsaturated six-

Table 1 Anti-CVB3 activity and cytotoxicity in Vero cells for compound **1** and its 16 diastereoisomers and 16 regioisomers[a]

			Configuration				
Groups	Compounds	CEs[b]	A ring	D ring	TC_{50}[c] (μM)	IC_{50} (μM)	SI[d]
	1	(−)	4*R*,11*R*	16*R*,18*R*,24*R*,26*S*	11.1 ± 1.5	2.1 ± 1.1	5.2
A	**19**	(−)	4*R*,11*R*	16*R*,18*R*,24*R*,26*R*	57.7 ± 5.4	>33.3	—[e]
	20	(+)	4*S*,11*S*	16*S*,18*S*,24*S*,26*S*	57.7 ± 2.8	>33.3	—[e]
	21	(+)	4*S*,11*R*	16*R*,18*R*,24*R*,26*R*	57.7 ± 9.1	33.3 ± 4.2	1.7
	22	(−)	4*R*,11*S*	16*S*,18*S*,24*S*,26*S*	57.7 ± 5.3	>33.3	—[e]
	23	(+)	4*S*,11*S*	16*R*,18*R*,24*R*,26*R*	48.1 ± 5.2	11.1 ± 2.5	4.3
	24	(−)	4*R*,11*R*	16*S*,18*S*,24*S*,26*S*	48.1 ± 6.3	>11.1	—[e]
	25	(−)	4*R*,11*S*	16*R*,18*R*,24*R*,26*R*	57.7 ± 7.0	33.3 ± 2.2	1.7
	26	(+)	4*S*,11*R*	16*S*,18*S*,24*S*,26*S*	57.7 ± 6.6	>33.3	—[e]
B	**27**	(+)	4*S*,11*R*	16*S*,18*R*,24*R*,26*S*	>100.0	>33.3	—[e]
	28	(−)	4*R*,11*S*	16*R*,18*S*,24*S*,26*R*	>100.0	>33.3	—[e]
	29	(−)	4*R*,11*R*	16*S*,18*R*,24*R*,26*S*	48.1 ± 5.2	>11.1	—[e]
	30	(+)	4*S*,11*S*	16*R*,18*S*,24*S*,26*R*	23.1 ± 4.2	>11.1	—[e]
	31	(−)	4*R*,11*S*	16*S*,18*R*,24*R*,26*S*	57.7 ± 1.0	22.6 ± 3.3	2.6
	32	(+)	4*S*,11*R*	16*R*,18*S*,24*S*,26*R*	100.0 ± 8.8	33.3 ± 2.9	3.0
	33	(+)	4*S*,11*S*	16*S*,18*R*,24*R*,26*S*	48.1 ± 4.4	>11.1	—[e]
	34	(−)	4*R*,11*R*	16*R*,18*S*,24*S*,26*R*	57.7 ± 2.4	>33.3	—[e]
C	**35**	(−)	4*R*,11*R*	16*R*,18*R*,24*R*,26*R*	23.1 ± 4.1	11.11 ± 1.35	2.1
	36	(+)	4*S*,11*S*	16*S*,18*S*,24*S*,26*S*	33.3 ± 3.2	>11.11	—[e]
	37	(+)	4*S*,11*R*	16*R*,18*R*,24*R*,26*R*	19.3 ± 3.7	11.1 ± 2.3	1.7
	38	(−)	4*R*,11*S*	16*S*,18*S*,24*S*,26*S*	19.3 ± 2.4	>11.1	—[e]
	39	(+)	4*S*,11*S*	16*R*,18*R*,24*R*,26*R*	16.0 ± 2.2	3.7 ± 1.2	4.3
	40	(−)	4*R*,11*R*	16*S*,18*S*,24*S*,26*S*	16.0 ± 1.8	>3.7	—[e]
	41	(−)	4*R*,11*S*	16*R*,18*R*,24*R*,26*R*	19.3 ± 4.1	8.6 ± 1.3	2.2
	42	(+)	4*S*,11*R*	16*S*,18*S*,24*S*,26*S*	48.1 ± 6.2	8.6 ± 1.5	5.6
D	**43**	(+)	4*S*,11*R*	16*S*,18*R*,24*R*,26*S*	>100.0	>33.3	—[e]
	44	(−)	4*R*,11*S*	16*R*,18*S*,24*S*,26*R*	>100.0	>33.3	—[e]
	45	(−)	4*R*,11*R*	16*S*,18*R*,24*R*,26*S*	57.7 ± 6.9	>33.3	—[e]
	46	(+)	4*S*,11*S*	16*R*,18*S*,24*S*,26*R*	57.7 ± 5.2	>33.3	—[e]
	47	(−)	4*R*,11*S*	16*S*,18*R*,24*R*,26*S*	48.1 ± 4.1	11.11	4.3
	48	(+)	4*S*,11*R*	16*R*,18*S*,24*S*,26*R*	57.7 ± 4.4	>33.3	—[e]
	49	(+)	4*S*,11*S*	16*S*,18*R*,24*R*,26*S*	69.3 ± 8.0	>33.3	—[e]
	50	(−)	4*R*,11*R*	16*R*,18*S*,24*S*,26*R*	69.3 ± 3.3	33.3	2.1
	Ribavirin[f]	—			8196.7 ± 45.6	1577.5 ± 84.4	5.2
	Pleconaril[f]	—			40.5 ± 2.6	2.9 ± 0.5[g]	14045.1

[a] TC_{50} and IC_{50} data represent the mean values for three independent determinations. [b] Cotton effects at λ_{max} 255 nm. [c] Cytotoxic concentration required to inhibit Vero cell growth by 50%. [d] The SI value equaled TC_{50}/IC_{50}. [e] The SI could not be determined under the test conditions. [f] Positive control. [g] nM.

membered ketone ring; (4) a series of substitution reactions and aromatic Claisen rearrangements to introduce the side chain; and (5) tandem oxidative dearomatization/cyclization to produce the 5–6 oxaspiro moiety. X-ray crystallography studies confirmed the structures of the intermediates and one final diastereoisomer product. The photochemical Diels–Alder reaction was shown to be an unusual *trans*-selective cycloadditon, which broke the common Diels–Alder reaction rule and a 100% *trans*-fused product was obtained. This has been completely evidenced, by density functional theory calculations, to be due to the unreactivity of the *cis*-cycloheptenone in cycloadditon.

Conclusions

In summary, we obtained 16 diastereoisomers and 16 regioisomers of novel skeleton natural product spirooliganin in total with 2.23% overall yield, in which the isomerization derived from the non-selective UV-promoted Diels–Alder cycloaddition and the regioselective thermal hetero-Diels–Alder reaction. The structures of all the synthesized compounds were unambiguously assigned by comprehensive analysis of spectroscopic data, especially 2D NMR, ECD analysis and modified Mosher's method. By such a library construction of the diverse isomers of **1**, we were able to investigate the effect of regio and stereo configuration on the bioactivity of the whole structure. Preliminary biological evaluation revealed the essential role of the D-ring 16*R*,18*R*,24*R*, and 26*R* configuration for their antiviral activity in both diastereoisomers and regioisomers. Spirooliganin **1** and regioisomer **39** have been screened as potent inhibitors against CVB3 for further mechanism study, which will be published in due course. This work not only gives a good example of how to construct a stereoisomers library for complex natural product containing multiple chiral centers for investigating their SSAR, but is also of great benefit to the construction of 6–6–6–7 skeleton compounds in organic synthesis. The unusual and confirmed photo-induced *trans*-Diels–Alder

reaction in this study has certain implications for the synthesis of other analogs with a similar *trans*-cycloaddition moiety.

Author contributions

S.-S. Y. initiated the project. S.-S. Y., S.-G. M., K.·N.·H., J. Q., and R.-B. W. designed the experiments. S.-G. M. isolated the new spirooliganin (**1**) and elucidated all compounds, and crystallized synthetic intermediate samples and final products. R.-B. W. synthesized all compounds. S.-G. M., R.-B. W., J. Q., Y.-B. L., Y. L., and X.-J. W. performed compound isolation and characterization. K. N. H. and C.·S. J. performed the computational analysis. R.-M. G. and Y.-H. L. performed *in vitro* experiments. All authors analysed and discussed the results. S.-G. M., R.-B. W., K.·N.·H., J. Q., and S.-S. Y. prepared the manuscript. R.-B. W., S.-G. M., and C.·S. J. contributed equally to this work.

Conflicts of interest

There are no conflicts to declare.

Acknowledgements

This work was supported by grants from the National Natural Science Foundation of China (no. 21732008, 21672261 and 82073739), the CAMS Innovation Fund for Medical Sciences (no. 2016-I2M-3-010), and the National Mega-project for Innovative Drugs (no. 2018ZX09711001-008-001). We are grateful to the Department of Instrumental Analysis of our institute for the acquisition of the IR, NMR, and MS spectra, and to the State Key Laboratory of Natural and Biomimetic Drugs of Peking University and the Instrumental Analysis Center of Beijing University of Chemical Technology for the X-ray crystallographic measurements and analyses.

Notes and references

1 D. P. Curran, Q. Zhang, C. Richard, H. Lu, V. Gudipati and C. S. Wilcox, *J. Am. Chem. Soc.*, 2006, **128**, 9561–9573.
2 S. C. Sinha, A. Sinha, A. Yazbak and E. Keinan, *J. Org. Chem.*, 1996, **61**, 7640–7641.
3 C. S. Wilcox, V. Gudipati, H. Lu, S. Turkyilmaz and D. P. Curran, *Angew. Chem., Int. Ed.*, 2005, **44**, 6938–6940.
4 S. Das, L.-S. Li, S. Abraham, Z. Chen and S. C. Sinha, *J. Org. Chem.*, 2005, **70**, 5922–5931.
5 P. Das, P. Babbar, N. Malhotra, M. Sharma, G. R. Jachak, G. Rajesh, R. G. Gonnade, D. Shanmugam, K. Harlos, M. Yogavel, A. Sharma and D. S. Reddy, *J. Med. Chem.*, 2018, **61**, 5664–5678.
6 S. D. Edmondson and S. J. Danishefsky, *Angew. Chem., Int. Ed.*, 1998, **37**, 1138–1140.
7 S. Edmondson, S. J. Danishefsky, L. Sepp-Lorenzino and N. Rosen, *J. Am. Chem. Soc.*, 1999, **121**, 2147–2155.
8 F. V. Nussbaum and S. J. Danishefsky, *Angew. Chem., Int. Ed.*, 2000, **39**, 2175–2178.
9 S. Singh, *Chem. Rev.*, 2000, **100**, 925–1024.
10 J. D. Moretti, X. Wang and D. P. Curran, *J. Am. Chem. Soc.*, 2012, **134**, 7963–7970.
11 D. P. Curran, M. K. Sinha, K. Zhang, J. J. Sabatini and D. H Cho, *Nat. Chem.*, 2012, **4**, 124–129.
12 J. Ding and D. G. Hall, *Angew. Chem., Int. Ed.*, 2013, **52**, 8069–8073.
13 M. T. Oliveira, M. Luparia, D. Audisio and N. Maulide, *Angew. Chem., Int. Ed.*, 2013, **52**, 13149–13152.
14 M. A. Schafroth, G. Zuccarello, S. Krautwald, D. Sarlah and E. M. Carreira, *Angew. Chem., Int. Ed.*, 2014, **53**, 13898–13901.
15 S. Krautwald and E. M. Carreira, *J. Am. Chem. Soc.*, 2017, **139**, 5627–5639.
16 S. G. Ma, W. Z. Tang, Y. X. Liu, Y. C. Hu, S. S. Yu, Y. Zhang, X. G. Chen, J. Qu, J. H. Ren, Y. B. Liu, S. Xu, Y. Y. Liu, Y. Li, H. N. Lü and X. F. Wu, *Phytochemistry*, 2011, **72**, 115–125.
17 W. Z. Tang, S. G. Ma, J. Qu, S. S. Yu, Y. B. Liu, D. M. Su and J. Liu, *J. Nat. Prod.*, 2011, **74**, 1268–1271.
18 S. G. Ma, Y. Gao, H. Q. Wang, L. Li, Y. B. Liu, J. Qu, Y. Li, S. Xu, H. N. Lv, Y. H. Li and S. S. Yu, *Tetrahedron*, 2016, **72**, 3003–3013.
19 S. G. Ma, R. M. Gao, Y. H. Li, J. D. Jiang, N. B. Gong, L. Li, Y. Lü, W. Z. Tang, Y. B. Liu, J. Qu, H. N. Lü, Y. Li and S. S. Yu, *Org. Lett.*, 2013, **15**, 4450–4453.
20 S. K. Chen, H. Li and P. Y. Chen, *Flora of China*, Science Press, Beijing, 1996, vol. 30, p. 224.
21 L. Y. Song, H. L. Yao and R. B. Tong, *Org. Lett.*, 2014, **16**, 3740–3743.
22 K. Takao, S. Noguchi, S. Sakamoto, M. Kimura, K. Yoshida and K. Tadano, *J. Am. Chem. Soc.*, 2015, **137**, 15971–15977.
23 N. Zhao, X. D. Ren, J. H. Ren, H. N. Lü, S. G. Ma, R. M. Gao, Y. H. Li, S. Xu, L. Li and S. S. Yu, *Org. Lett.*, 2015, **17**, 3118–3121.
24 M. T. Allingham, E. L. Bennett, D. H. Davies, P. M. Harper, A. Howard-Jones, Y. T. H. Mehdar, P. J. Murphy, D. A. Thomas, P. W. R. Caulkett, D. Potter, C. M. Lam and A. C. O'Donoghue, *Tetrahedron*, 2016, **72**, 496–503.
25 H. M. L. Davies, Ø. Loe and D. G. Stafford, *Org. Lett.*, 2005, **7**, 5561–5563.
26 J. Nikolai, Ø. Loe, P. M. Dominiak, O. O. Gerlitz, J. Autschbach and H. M. L. Davies, *J. Am. Chem. Soc.*, 2007, **129**, 10763–10772.
27 L. Wei, M. X. Xiao and Z. X. Xie, *Org. Lett.*, 2014, **16**, 2784–2786.
28 J. W. Zhang, Q. Q. Jiang, D. J. Yang, X. M. Zhao, Y. L. Dong and R. H. Liu, *Chem. Sci.*, 2015, **6**, 4674–4680.
29 Y. F. Liang, S. Song, L. S. Ai, X. W. Li and N. Jiao, *Green Chem.*, 2016, **18**, 6462–6467.
30 F. Schoenebeck, D. H. Ess, G. O. Jones and K. N. Houk, *J. Am. Chem. Soc.*, 2009, **131**, 8121–8133.
31 J. A. Marshall, *Acc. Chem. Res.*, 1969, **2**, 33–40.
32 K. N. Houk, L. N. Domelsmith, R. W. Strozier and R. T. Patterson, *J. Am. Chem. Soc.*, 1978, **100**, 6531–6533.
33 R. W. Strozier, P. Caramella and K. N. Houk, *J. Am. Chem. Soc.*, 1979, **101**, 1340–1343.
34 Y. X. Wang, Y. H. Li, Y. H. Li, R. M. Gao, H. Q. Wang, Y. X. Liu, L. M. Gao, Q. N. Lu, J. D. Jiang and D. Q. Song, *Bioorg. Med. Chem. Lett.*, 2011, **21**, 5787–5790.